SETAC PRESS

MOLECULAR SIMULATION OF A MODEL OF DISSOLVED ORGANIC MATTER

Rebecca Sutton,*† Garrison Sposito,† Mamadou S. Diallo,‡§ and Hans-Rolf Schulten∥
†Division of Ecosystem Sciences, University of California at Berkeley, Berkeley, California 94720-3114, USA
‡Materials and Process Simulation Center, Beckman Institute, California Institute of Technology, Pasadena, California 91125, USA
§Department of Civil Engineering, Howard University, Washington, DC 20059, USA
∥University of Rostock, Institute of Soil Science and Plant Nutrition, Justus-von-Liebig-Weg 6, D-18059 Rostock, Germany

Abstract—A series of atomistic simulations was performed to assess the ability of the Schulten dissolved organic matter (DOM) molecule, a well-established model humic molecule, to reproduce the physical and chemical behavior of natural humic substances. The unhydrated DOM molecule had a bulk density value appropriate to humic matter, but its Hildebrand solubility parameter was lower than the range of current experimental estimates. Under hydrated conditions, the DOM molecule went through conformational adjustments that resulted in disruption of intramolecular hydrogen bonds (H-bonds), although few water molecules penetrated the organic interior. The radius of gyration of the hydrated DOM molecule was similar to those measured for aquatic humic substances. To simulate humic materials under aqueous conditions with varying pH levels, carboxyl groups were deprotonated, and hydrated Na^+ or Ca^{2+} were added to balance the resulting negative charge. Because of intrusion of the cation hydrates, the model metal–humic structures were more porous, had greater solvent-accessible surface areas, and formed more H-bonds with water than the protonated, hydrated DOM molecule. Relative to Na^+, Ca^{2+} was both more strongly bound to carboxylate groups and more fully hydrated. This difference was attributed to the higher charge of the divalent cation. The Ca-DOM hydrate, however, featured fewer H-bonds than the Na-DOM hydrate, perhaps because of the reduced orientational freedom of organic moieties and water molecules imposed by Ca^{2+}. The present work is, to our knowledge, the first rigorous computational exploration regarding the behavior of a model humic molecule under a range of physical conditions typical of soil and water systems.

Keywords—Humic substances   Molecular simulation   Cation binding   Dissolved organic matter

INTRODUCTION

Computational studies have provided insight regarding the adsorption mechanisms and diffusional behavior of significant environmental contaminants at or near mineral surfaces, such as radionuclides [1,2] and chlorinated organic compounds [3,4]. The dramatic effect of humic substances on the fate and transport of contaminants [5] also motivates the search for a mechanistic understanding of molecular reactions involving humic moieties. Recent experimental attempts (see, e.g., [5–9]) to elucidate the chemical behavior of humic substances in soil and water systems also may benefit from explorations using atomistic simulation, provided that appropriate molecular models for humic substances (effective model humic molecules) can be constructed. An effective model humic molecule, as defined in the present paper, is not necessarily a molecule that exists within an actual humic sample but, instead, is one that captures the structural and functional qualities observed experimentally and can provide insight regarding interaction mechanisms of interest.

Several effective model humic molecules have been studied using atomistic simulation. These include the humic molecule designed by Stevenson [5] through synthesis of a variety of experimental data regarding humic substances; the lignin-based humic building block proposed by Steelink [10] and its derivative, the Temple-Northeastern-Birmingham humic building block [11], which accounts for the polysaccharide and protein content of humic substances; the series of molecules created by Leenheer [12] and by Leenheer et al. [13,14] to

represent Suwannee River fulvic acid after review of considerable data regarding this particular humic fraction; the series of dissolved organic matter (DOM) molecules designed and refined by Schulten and Schnitzer [15] and by Schulten [16] based on pyrolysis and other experimental studies of natural organic matter; the oxidized lignin–carbohydrate complex simulated by Shevchenko and Bailey [17]; and the series of humic molecules constructed through computer-assisted structure elucidation by Diallo et al. [18,19] to represent the Chelsea Histosol humic acid. Molecular simulations using these model humic molecules rarely have emphasized validation with available experimental data on humic substances [16,17,20]. In addition, many simulations are performed under physical conditions inappropriate to soil and water systems: For example, studies may be limited to modeling humic molecules in the gas phase [16,20] or within completely dehydrated environments [18,19,21]. Even when hydrated, simulated model humic molecules often feature fully protonated carboxyl groups and, therefore, represent behavior only under extremely acidic solution conditions [11,22]. Finally, the use of generalized atomistic force fields unsuitable for detailed structural calculations regarding complex organic molecules, along with the use of inadequate modeling techniques, can lead to simulations of humic structures that inadequately model the conformation and functionality of natural humic materials [20,23].

To begin addressing deficiencies in existing atomistic simulations of effective model humic molecules, we present a series of calculations involving the widely used Schulten DOM molecule [16] within a range of physicochemical environments. This molecule is a particularly large and complex model of humic matter, and existing studies of it exhibit many of the

* To whom correspondence may be addressed
(rsutton@nature.berkeley.edu).

shortcomings described above (see, e.g., [16,22]). Bulk characteristics of this humic molecule were determined using a dry, densely packed system, whereas aqueous solution characteristics were determined through simulations representing dilute humic solutions under acidic (carboxyl groups) and near-neutral (carboxylate groups) pH conditions. To balance the resulting negative charge, the deprotonated humic polyanions were saturated with hydrated Na^+ or Ca^{2+} counter-ions. Subsequent data analysis provided estimates of physical and chemical characteristics that can be compared to available experimental data regarding humic substances.

The effective model humic molecule was described using the all-atom force-field Condensed-phase Optimized Molecular Potentials for Atomistic Simulation Studies (COMPASS; Accelrys, San Diego, CA, USA) [24]. Validation studies indicate that the COMPASS force field is capable of accurate prediction of structural and thermophysical properties for a broad range of organic and inorganic substances in both gaseous and liquid or solid states [25]. Studies contrasting structural and dynamic properties obtained from COMPASS with those obtained using other force fields or simulation methods also demonstrate the high quality of the COMPASS force field [26,27].

Two simulation algorithms were used to explore the properties of the DOM molecule as expressed by COMPASS. Energy minimization (EM) involves optimization of atomic coordinates to reduce the potential energy of a molecular system, as calculated by summing all interaction terms described by the force field [24]. Minimization algorithms are independent of temperature, and 0 K conditions are assumed. The molecular conformation adopted after minimization is one of many stable states that occupy local energy minima. To move a molecule from a conformation associated with a local energy minimum to one associated with the global energy minimum, representing the most stable state of a particular system, a minimized molecule may be subjected to further calculations using a molecular dynamics (MD) algorithm. The shift to a second modeling algorithm allows exploration of different molecular configurations that may approach the one associated with the global energy minimum. Molecular dynamics algorithms solve Newton–Euler equations of motion at an atomic scale, essentially simulating the movements of atoms or molecules as they interact with each other over time [28]. As the name suggests, MD also is an appropriate method for obtaining dynamic information from a model system.

MATERIALS AND METHODS

The COMPASS force field

The COMPASS force field includes two classes of interaction parameter [25]. Valence terms represent bond, angle, torsion angle, and out-of-plane (inversion) angle interactions as well as cross-coupling bond–bond, bond–angle, and bond–torsion interactions. Nonbond terms include van der Waals interactions, represented by a Lennard–Jones (6–9) function, and electrostatic interactions, represented by a Coulombic equation. To model accurately a broad variety of substances, the same elements in different chemical environments are classified as different COMPASS atom types, each with its own set of interaction constants [25]. Electrostatic interactions rely on partial charges, which are constructed through summation of values representing the charge separation between a particular atom and each of the surrounding atoms to which it is covalently bound [25]. The COMPASS valence parameters and

atomic partial charges were derived from quantum chemical data, whereas van der Waals parameters were determined by conducting MD simulations of molecular liquids and fitting simulated cohesive energies and equilibrium densities to experimental data [25]. As a result, the cohesive energies calculated from COMPASS nonbond interactions, using van der Waals and electrostatic parameters developed relative to a reference state of infinite separation of molecules, may be compared to experimentally determined intermolecular potential energy values. In contrast, COMPASS valence parameters were not optimized relative to a well-defined experimental state but, instead, were chosen based on their ability to provide appropriate equilibrium geometries and vibrational motions [25]. Total potential energies calculated using the COMPASS force field include nonbond and valence contributions, and they can be compared to one another but not to experimental measurements of potential energy.

Simulation of the Schulten DOM molecule

The DOM molecule that we investigated consisted of a Schulten humic acid molecule covalently bonded to a hexapeptide and a trisaccharide. It contained 1,157 atoms, with the molecular formula $C_{447}H_{421}O_{272}N_{15}S_2$ and a molar mass of 10,419.3 g/mol. A cyclic dinitrogen functional group in the original Schulten molecule was changed from 1H-pyrazole to imidazole, because the latter is a common substituent on organic molecules, such as DNA, and therefore is more likely to exist in humic materials [5]. The COMPASS force field does not contain charge distribution information for 13 of the DOM bonds: 10 C-O bonds between oxygenated functional groups (alcohol, ether, ester) substituted to *p*-benzoquinone units; 2 C-N bonds between primary amines bonded to the same C, which in turn was double-bonded to N; and 1 C-C bond between neighboring ketone groups. Because the force field was not designed to include these bonds, partial charges for these 26 atoms were inaccurate, although their contribution to the DOM molecule is negligible. The missing bonds lacked valence parameters, necessitating inspection for physically unrealistic behavior during the course of calculations.

The following simulation procedure, based on that outlined by Diallo et al. [18], was designed to determine whether the model molecule could produce realistic values for dry bulk density and the Hildebrand solubility parameter (defined below). First, a packing procedure involving both EM and MD calculations was used to adjust the density of the DOM molecule. The procedure began with minimization of a nonperiodic DOM system using the Cerius2 Smart Minimizer (Accelrys) and high-level convergence criteria [24]. The three-dimensional Ewald summation method [28] was used to calculate electrostatic interactions (real-space cutoff, 9 Å; reciprocal space cutoff, 3 Å^{-1}), whereas direct summation was used to determine van der Waals interactions, using a real-space cutoff of 9 Å. The energy-minimized DOM structure was inserted into a periodic cell at a density of 0.50 g/cm^3. The periodic system was subjected to an EM-annealing MD-EM sequence: EM was followed by MD (with number of atoms, simulation cell volume, and temperature constant; *NVT* ensemble) calculations using the Berendsen method of temperature control (relaxation constant, 0.1 picosecond [ps]) [28], a 0.5-femtosecond time step, and initial velocities assigned using a Maxwell–Boltzmann distribution centered at 300 K. A complete annealing cycle was performed from 300 to 600 K and back, using 30,000 steps (15 ps) at each 100 K stage. Final atom

positions and velocities from each preceding annealing stage were used as initial input for the next stage. The annealing cycle ended at 400 K, so a final MD (*NVT* ensemble) simulation of 15 ps at 300 K brought the system back to its initial temperature. A minimization completed this sequence.

The cell dimensions of the periodic DOM system were reduced to yield a density of 0.60 g/cm^3, and a second EM-annealing MD-EM sequence was performed, using 10 ps at each annealing stage. This sequence was repeated for the densities 0.70, 0.85, 1.0, 1.15, and 1.25 g/cm^3. After the packing procedure, MD (with number of atoms, pressure, and temperature constant; *NPT* ensemble) simulation for 50 ps using the Andersen pressure-control method (0.0001 GPa; cell mass prefactor, 0.04) [28] allowed the DOM system to achieve a bulk density appropriate for a temperature of 300 K through variation of cell dimensions, and subsequent EM provided the optimized organic structure.

The density, molecular volume, solvent-accessible Connolly surface area (solvent molecule radius, 1.4 Å) [24], and dipole moment were calculated for the final configuration of the DOM molecule. The simulation cell volume occupiable by solvent molecules with 1.4 Å radii was calculated as well. Hydrogen bonds were determined for periodic and nonperiodic DOM systems using a maximum H-acceptor distance of 1.8 Å and a minimum donor-H-acceptor angle of 120° [29]. The total potential energy, a relative value, was obtained through summation of the energy contributions of all valence and nonbond interactions present in the dry, densely packed DOM system. Determination of the gas-phase strain energy, or the potential energy of the DOM molecule in a nonperiodic environment, provided information for calculation of the Hildebrand solubility parameter:

$$\delta = \sqrt{\frac{-(E_p - E_{np})}{N_A V_p}} \tag{1}$$

where E_p is the condensed (solid or liquid) phase (periodic) potential energy, E_{np} is the gas phase (nonperiodic) potential energy (the cohesive energy is obtained through subtraction of E_{np} from E_p), N_A is Avogadro's number, and V_p is the cell volume [18]. Because the Ewald summation method cannot be used for nonperiodic systems [28], a cubic spline-switching method ($r_{on} = 20.0$ Å, $r_{off} = 21.0$ Å) was used to sum electrostatic and van der Waals contributions to the potential energy of the nonperiodic DOM molecule [24]. The modeling data then were compared to simulation results published by Schulten [16] as well as to available experimental measurements. Because all properties of the model DOM were derived from a single configuration of this molecule, standard deviations associated with these data are not available.

Solvation of the Schulten DOM molecule

A model humic molecule must be able to mimic the behavior of humic substances in hydrated environments typical of natural soil and water systems. Simulations of the DOM molecule under conditions resembling dilute aqueous solution provided information concerning the interactions of this model organic material with water molecules. To simulate DOM within a near-neutral pH environment, the molecule's carboxyl groups were deprotonated to form carboxylates, and the resulting negative charge was balanced with Na$^+$. Despite the preference of carboxylate groups for more highly charged metal cations [6], to our knowledge the literature contains no previous simulations of a humic polyanion saturated with di-

valent metal cations (e.g., Ca^{2+}). An assessment of the COMPASS water model preceded studies of the DOM molecule under hydrated and deprotonated, Na- or Ca-saturated conditions to assure that the force field produced no unusual bulk solvent behavior.

Bulk water system. A periodic cell measuring 20.000 Å on each side was filled with 267 water molecules, with initial O-H bond lengths of 0.9572 Å and H-O-H angles of 104.52° [30], producing a density of 0.998 g/cm^3. An EM-annealing MD-EM sequence was performed using the parameters described above but with 10,000 steps (5 ps) at each 100 K stage. The final configuration was used as input for 25 ps of MD (*NVT* ensemble) calculations at 300 K. Average potential energies were divided by the number of water molecules in the simulation cell to determine energy values per mole of water. The first 2 ps of the MD run were ignored, because the system temperature had not reached 300 K during this period. The distributions of bond lengths and angles and the number of H-bonds present were determined. Comparisons of simulation data to experimental measurements of bulk water properties are provided below. Further comparison with the three most common and effective water models used in simulations of hydrated mineral and organic systems is supplied by Sutton [30].

The total potential energy of COMPASS water at 300 K is -35.47 ± 0.26 kJ/mol. The cohesive energy, or the intermolecular potential energy arising from nonbond (van der Waals and electrostatic) interactions, is -41.87 ± 0.67 kJ/mol, a value that compares favorably with the experimentally determined intermolecular potential energy of water (-41.4 kJ/mol) [31]. The average O-H bond length of 0.975 ± 0.026 Å for the COMPASS water molecule was similar to the empirical value of 0.98 Å for liquid water at 25°C [32]. However, the average COMPASS H-O-H bond angle of $99.90 \pm 4.66°$ was smaller than the 105.4° measured experimentally [32]. This indicates that a bias favoring smaller H-O-H bond angles, perhaps taking the form of weak H-H repulsion or strong angular force, is inherent to the COMPASS force field. A H-O-H bond angle substantially reduced from that of a strictly tetrahedral conformation (109.5°) is likely to inhibit the formation of networks of H-bonds within the model water system. Only 47 H-bonds existed after MD simulation at 300 K, just 9% of those possible for an idealized tetrahedral network featuring 267 molecules [30]. Although the small average bond angle of the COMPASS water molecule reduced its ability to form H-bonded networks within bulk solution, this geometric property was not expected to inhibit the formation of H-bonds between water and organic or mineral functional groups.

Hydrated DOM molecule. Using InsightII V2000.1 (Accelrys), 733 water molecules were arranged around the dry, densely packed DOM molecule, forming a solvation layer with a thickness of 5 Å. This hydrated DOM system was nonperiodic, designed to simulate the structure of the organic molecule in a dilute solution. It was subjected to minimization and then to four annealing MD-EM sequences, with calculations representing 20 ps for each temperature stage. The cubic spline-switching method was used to sum electrostatic and van der Waals energy contributions. Afterwards, a MD (*NVT* ensemble) calculation of 50 ps at 300 K was followed by a final minimization, providing a well-minimized structure for the DOM hydrate. Calculation of potential energy and volume was performed for the final configuration of the DOM hydrate, both with and without associated water molecules. The molar po-

tential energy of water molecules was determined by subtracting the potential energy of the DOM molecule in its hydrated configuration, but without associated water molecules, from the potential energy of the hydrated DOM system and then dividing this value by the number of water molecules present. The solvent-accessible surface area and dipole moment of the DOM molecule were calculated as well. Because all these properties were associated with a single system realization, standard deviations are not available for the values calculated. Cerius[2] provided the radius of gyration of the organic molecule. Intra- and intermolecular H-bonds were enumerated as described above.

Deprotonated, Na-saturated DOM hydrate. Published methods for modeling deprotonated, Na-saturated organic molecules have ignored the hydration state of Na^+ [33–35], despite experimental evidence indicating that these cations are octahedrally coordinated in aqueous solution [36]. Presented here is a novel simulation technique designed to titrate the DOM molecule with hydrated Na^+ in a stepwise fashion. Eleven carboxyl H atoms were removed from exterior locations of the final dry DOM conformation. Atom type and charge adjustments provided by the COMPASS force field recognized these modified functional groups as carboxylates. Eleven energy-minimized Na^+-$6H_2O$ hydrates were placed near the carboxylates such that both Na-carboxylate O distances were near 5.2 ± 0.2 Å (5.2 Å being the length of one Na^+ radius, an interceding [water] O diameter, and one [carboxylate] O radius [http://www.webelements.com]). The nonperiodic system was subjected to an EM-annealing MD-EM sequence, with MD calculations representing 10 ps at each temperature stage. These steps were repeated six times, with deprotonation moving from exterior to interior carboxyl groups to emulate the process of exchange postulated by von Wandruszka et al. [37], until all 77 carboxyl groups were transformed into carboxylates associated with Na-hydrates. Occasionally, cramped conditions in the interior region of the DOM molecule required shorter initial Na-carboxyl O distances of approximately 4 Å.

InsightII was used to coat the Na-DOM structure with a layer (thickness, 5 Å) of water. With the 1,272 water molecules composing this hydration shell, a total of 1,734 water molecules were now present in the Na-DOM hydrate. An EM-annealing MD-EM sequence with 5 ps for each annealing stage was performed to equilibrate the system. This was followed by a MD (*NVT* ensemble) simulation of 50 ps at 300 K and a final EM calculation. Data analyses for the final configuration of the hydrated Na-DOM structure, as well as for the dehydrated organic polyanion, were performed as described above. The radius of gyration was calculated for the Na-DOM structure without associated water molecules or cations, because the small angle x-ray scattering methods typically used to measure this property experimentally are capable of time resolution on the order of 10^{-3} s [38] while electrostatic associations involving water or cations typically have residence times of 10^{-7} s or less [39]. Radial distribution functions (RDFs; represented mathematically as $g_{\alpha\beta}[r]$) for Na-total O, Na-water O, and Na-carboxylate O atom pairs were calculated using a cutoff distance of 9 Å, a bin interval of 0.1 Å, and the following equation:

$$\mathrm{d}n_{\alpha\beta} = 4\pi\frac{N_\beta}{V}g_{\alpha\beta}(r)r^2\mathrm{d}r \tag{2}$$

where $\mathrm{d}n_{\alpha\beta}$ is the average number of β species atoms (out of a total of N_β) within a spherical shell of radius r and thickness
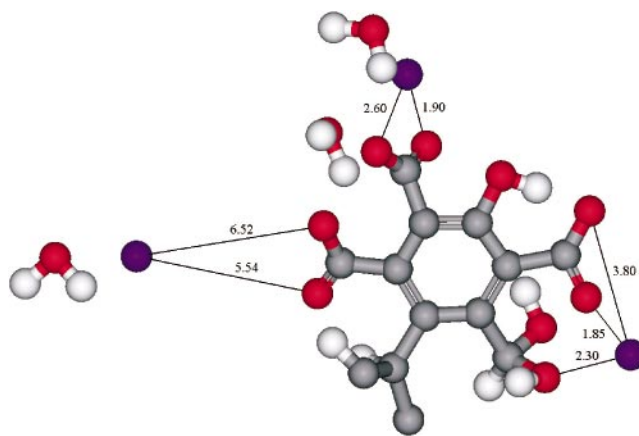
Fig. 1. A portion of the Na-dissolved organic matter structure featuring an outer-sphere Na–carboxylate complex (left), a doubly inner-sphere Na–carboxylate complex (top), and a singly inner-sphere Na–carboxylate complex, which also happens to possess inner-sphere coordination with an alcohol group (right). Gray spheres represent C, red spheres O, white spheres H, and purple spheres Na^+. Measurements indicate distances between atoms (Å).

dr centered on an α species atom [40]. For nonperiodic systems, V is defined as 1 Å^3, and as r approaches a value equal to half that of the longest dimension of the system, $g_{\alpha\beta}(r)$ is made to approach zero, without the use of mathematical means of normalization. The coordination number (CN) values, which in this case represent the average number of O atoms surrounding a cation within a radius (ρ) defined by the first minimum of the cation total-O RDF, were calculated for each RDF using the following equation:

$$\mathrm{CN}_{\alpha\beta}(\rho) = 4\pi\frac{N_\beta}{V}\int_0^\rho g_{\alpha\beta}(r)r^2\,\mathrm{d}r \tag{3}$$

Integration was accomplished using the trapezoidal rule in Matlab® (V5.3; MathWorks, Natick, MA, USA). The local environment of each cation was evaluated to determine the nature of its association with the DOM molecule and the type of carboxylate groups involved. To be considered part of an inner-sphere complex, a carboxylate O must be within the distance ρ, defined by the first RDF Na-O peak as being consistent with inner-sphere complexation. An ion was defined as singly inner-sphere coordinated when it was within the ρ distance for only one of the carboxylate O and as doubly inner-sphere coordinated when it was within the ρ distance for both carboxylate O (Fig. 1). An ion was defined as outer-sphere coordinated when the O of the nearest carboxylate groups were outside the ρ value. In addition, each cation was examined for signs of exchange movement, defined as movement away from the carboxylate group near which it was placed originally and toward a different carboxylate group.

Deprotonated, Ca-saturated DOM hydrate. The titration procedure outlined above was modified for simulation of a Ca-DOM hydrate. Eleven pairs of adjacent carboxyl groups on the exterior of the dry DOM molecule were deprotonated, providing a total of 22 carboxylate groups. Eleven energy-minimized Ca^{2+}-$6H_2O$ hydrates were placed near each carboxylate pair such that the shorter of the Ca-carboxylate O distances of each carboxylate was approximately 5.2 Å (the length of one Ca^{2+} radius, an interceding [water] O diameter, and one [carboxylate] O radius [http://www.webelements.com]). An EM-annealing MD-EM sequence was performed as
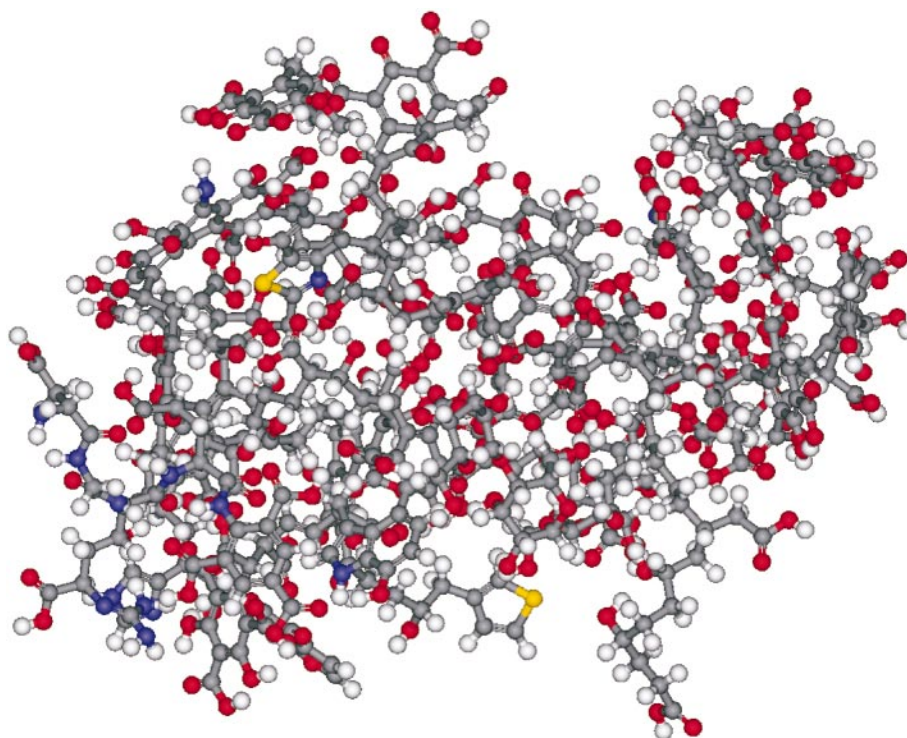
Fig. 2. The dry, densely packed dissolved organic matter molecule. Gray spheres represent C, red spheres O, white spheres H, blue spheres N, and yellow spheres S.

described above. These steps were repeated three times, beginning with exterior carboxyl groups and moving inward. During the fourth titration step, only 10 carboxylate groups were created, and five Ca^{2+} were added, for a total of 38 Ca^{2+}. One of these Ca^{2+} was placed just 3 Å from carboxylate O within the crowded interior environment. To maintain charge balance, one of the 77 carboxyl groups of the DOM molecule was not deprotonated. This carboxyl group was located at the end of an alkyl fragment that may be described as 2-pentenoic acid, which has the highest dissociation constant (~4.72 [41]) of any isolated carboxyl-containing molecular fragments in the DOM molecule. After titration, the Ca-DOM structure was hydrated with 994 water molecules, for a total of 1,222 water molecules in the system, and subjected to the same calculations and analyses described for the Na-DOM system.

RESULTS AND DISCUSSION

Energetic and structural properties of the DOM molecule

The total potential energy of the Schulten DOM molecule under dry, densely packed conditions was -1.809×10^4 kJ/mol (potential energy contributions [kJ/mol]: electrostatic, -1.328×10^4; van der Waals, -324.8; bond, 668.6; angle, 2,604; torsion, $-6,826$; inversion, 54.65; cross-term, -982.2). The gas-phase potential (strain) energy of the dry, densely packed DOM molecule was -1.527×10^4 kJ/mol. The Hildebrand solubility parameter (Eqn. 1), calculated from the difference in potential energies of the DOM molecule in periodic and nonperiodic states, therefore was 19.2 $J^{1/2}$ cm$^{-3/2}$, just below the range of experimental estimates, (20.5–27.6 $J^{1/2}$ cm$^{-3/2}$) [18]. Kopinke et al. [42] considered the solubility parameter to be an indication of polarizability. The solubility parameter calculated here thus suggests that the DOM molecule, as represented by the COMPASS force field, may be somewhat less polar, or more hydrophobic, than natural humic

substances [18]. Despite a potentially reduced polarity, the minimized DOM molecule exhibited 47 intramolecular H-bonds as well as 41 intermolecular H-bonds, the latter indicating substantial interaction with periodic reflections of the molecule. The nonperiodic DOM molecule described by Schulten [16] had only 24 intramolecular H-bonds, likely because of the less dense configuration. The dipole moment of the minimized molecule is 44.4 D, indicating organization of dipoles within the model DOM. It is possible that dipole–dipole interactions formed between the central DOM molecule and its densely packed periodic images [28].

The final configuration of the DOM molecule (Fig. 2) featured a bulk density of 1.36 g/cm³, within the range of experimental estimates (1.2–1.4 g/cm³) for the dry bulk density of humic substances [18]. The DOM model had a solvent-accessible surface area of 4,397.0 Å², approximately 1,000 Å² smaller than the area provided by Schulten [16] for a similar DOM configuration that included 35 water molecules and that had not been subjected to a packing procedure. The volume of the dry, densely packed DOM molecule was 8,190.4 Å³, marginally smaller than that documented by Schulten [16] for the partially hydrated DOM configuration. A third of the total periodic cell volume was empty, but only 6% of the cell volume was occupiable by probe molecules with radii of 1.4 Å, according to Cerius² volume calculations. The dry, densely packed DOM molecule therefore has a limited capacity to absorb guest species.

Energetic and structural properties of solvated DOM systems

The utility of a model humic molecule depends on its ability to mimic the behavior of humic substances under conditions relevant to soil and water environments—conditions that are invariably hydrated and rarely acidic enough to encourage full

Table 1. Properties of the protonated and deprotonated, cation-saturated dissolved organic matter (DOM) molecules

	H-DOM	Na-DOM	Ca-DOM
Surface area (Å^2)	4,415.4	5,731.4	5,638.6
Volume (Å^3)	8,233.9	8,033.1	8,037.1
Porosity	0.637	0.815	0.753
Radius of gyration (Å)	12.76	13.28	13.26
Dipole moment (D)	42.5	273.0	210.1
Water potential energy[a] (kJ/mol)	−333.4	−400.2	−401.6
H-bonds			
Total	28	109	61
Intramolecular	15	20	17
DOM-water	13	89	44

[a] These values cannot be compared to the molar potential energy of bulk water provided in *Materials and Methods* because of differences in simulation methodology.

protonation of carboxyl functional groups. Hydrated DOM systems investigated include the fully protonated species as well as deprotonated polyanions associated with hydrated Na^+ or Ca^{2+} counter-ions.

Hydrated DOM molecule. The total potential energy of the hydrated DOM molecule with associated water molecules was -2.560×10^5 kJ/mol, whereas the potential energy of the DOM molecule by itself was -1.158×10^4 kJ/mol. The latter potential energy is higher than that of the nonperiodic dry DOM molecule (-1.527×10^4 kJ/mol), suggesting that structural reorganization (necessary to optimize interactions with water) resulted in a configuration that was less suited to dehydrated conditions. The potential energy of the water molecules associated with the hydrated DOM was −333.4 kJ/mol (Table 1).

The dipole moment of the hydrated DOM molecule in isolation was 42.5 D (Table 1), similar to that of the dry, densely packed DOM molecule (44.4 D). The porosity of the hydrated DOM system, calculated as the volume ratio ($[V_{total} - V_{DOM}]/V_{total}$), was 0.637, whereas the solvent-accessible surface area of the DOM molecule in its hydrated conformation was 4,415.4 Å^2. The radius of gyration of the DOM molecule was 12.76 Å, well within the experimental range of 4.7 to 33 Å reported for aquatic humic substances [43,44] but less than the typical values of 30 to 100 Å reported for soil humic substances [45].

To accommodate its aqueous environment, the hydrated DOM adopted subtle structural changes, resulting in the reduction of intramolecular H-bonds and the appearance of DOM–water H-bonds. The hydrated DOM featured 15 intramolecular H-bonds and 13 H-bonds with water molecules, far fewer in total than the 47 intramolecular H-bonds observed in the dry DOM molecule. Graber and Borisover [46] suggested that on hydration, noncovalent links, such as H-bonds, between humic moieties would be disrupted as water molecules penetrated pores and hydrated polar organic functional groups. The results of this simulation indicate that penetration and hydration by water molecules may not be necessary to disrupt H-bonds between humic moieties, because water molecules did not enter interior regions of the DOM molecule during the course of the simulations. More DOM–water H-bonds would be expected if the added water molecules were able to penetrate the organic matrix rather than simply coating its external surface.

Deprotonated, Na- and Ca-saturated DOM hydrates. Energy-minimized, octahedrally coordinated Na^+ described by

the COMPASS force field featured a Na-O distance of 2.395 Å, whereas Ca^{2+} featured a Ca-O distance of 2.357 Å. The total potential energy of the Ca^{2+} hydrate was −1,036 kJ/mol, more than twice the total potential energy of the Na^+ hydrate (−449.9 kJ/mol), primarily because of a larger electrostatic contribution, given the divalent charge of the former, and the somewhat smaller cation-O distance.

The total potential energy of the Na-DOM hydrate was -7.262×10^5 kJ/mol, whereas that of the Ca-DOM hydrate was -5.585×10^5 kJ/mol. The total potential energy of the Na-saturated organic polyanion without associated water molecules was -3.233×10^4 kJ/mol, roughly threefold that of the fully protonated DOM hydrate structure without its associated water molecules (-1.158×10^4 kJ/mol). The Ca-saturated version of the polyanion had a total potential energy of -6.775×10^4 kJ/mol, approximately sixfold that of the protonated DOM molecule. The presence of carboxylate sites and compensating cations in the Na-DOM and Ca-DOM systems created electrostatic interactions, resulting in lower potential energies. Although the Ca-saturated system contained just under half the number of cations present in the Na-saturated system, the divalent charges on these cations resulted in a doubling of the potential energy found in the Ca-DOM conformation without associated water molecules as compared to Na-DOM. The potential energies of water molecules in the Na- and Ca-DOM hydrates were −400.2 and −401.6 kJ/mol, respectively (Table 1). The similarity of these values suggests that the effect of ion valence on the hydrophilicity of the cation-saturated polyanions was cancelled by variation in the number and arrangement of water molecules. These values are lower than that of water in the protonated DOM hydrate (−333.4 kJ/mol), indicating that the deprotonated, cation-saturated organic molecules were more hydrophilic than the protonated molecule. Dipole moments of 273.0 and 210.1 D calculated for the deprotonated organic structures within the Na-DOM and Ca-DOM hydrates, respectively, are much larger than the 42.5 D dipole moment calculated for the protonated DOM molecule, providing further evidence for the formation of a polar, hydrophilic environment with deprotonation. The slightly less negative charge of Ca-DOM (−76e) relative to Na-DOM (−77e) contributed to the reduced dipole moment of the former, as did subtle differences in conformation.

Porosities of 0.815 and 0.753 calculated for the Na- and Ca-DOM hydrates, respectively (Table 1), revealed a more porous organic structure than that seen for the protonated DOM molecule, with its porosity of 0.637. Insertion of fully hydrated cations within the organic matrices of the DOM molecule during titration triggered creation of intramolecular pores. The increase in hydrophilicity with deprotonation, indicated by the molar potential energies of water molecules associated with protonated and deprotonated versions of the DOM molecule, created conditions favorable to the maintenance of these water-filled pores. Molecular reconfiguration with pore formation produced expanded organic conformations with gyration radii of 13.28 and 13.26 Å for the Na- and Ca-DOM polyanions, respectively, relative to the value of 12.76 Å for the protonated DOM molecule. Surface areas likewise increased to 5,731.4 and 5,638.6 Å^2 for the Na- and Ca-DOM, respectively, relative to the value of 4,415.4 Å^2 for the protonated molecule. The creation of intramolecular pores and subsequent expansion of the deprotonated molecules influenced the porosity calculation by increasing the number of water molecules required to coat these cation-saturated polyanions to a depth of 5 Å and, thus,

increasing the total volumes of the simulation systems used to calculate porosity, from 2.266×10^4 Å^3 for the protonated molecule to 4.343×10^4 and 3.259×10^4 Å^3 for the Na- and Ca-DOM molecules, respectively. The difference in the total volumes of the simulation systems and, therefore, porosity for Na- and Ca-DOM is linked to the presence of fewer hydrated cations in the latter system. Reorganization into less compact structures containing many voids after deprotonation is consistent with atomic force microscopy images of dilute humic substances adsorbed to muscovites under aqueous conditions [47], which indicate that these natural organic molecules form dense clusters when influenced by acidic solutions and more elongated networks when surrounded by solutions close to neutral pH.

The Na-DOM system contained a total of 109 DOM H-bonds, or 20 intramolecular H-bonds and 89 H-bonds between the organic matter and associated water molecules (Table 1). The Ca-DOM system contained a total of 61 DOM H-bonds, or 17 intramolecular H-bonds and 44 DOM-water H-bonds (Table 1). Both systems displayed a dramatic increase in DOM–water H-bonds, relative to the protonated DOM system, which featured 13 such H-bonds (Table 1). This increase was linked to formation of water-filled pores within the DOM structures, which expanded the organic surface area available for interactions with water molecules. The Ca-DOM hydrate developed fewer H-bonds than the Na-DOM hydrate, because fewer water molecules were present. In addition, it is possible that the stronger electrostatic field produced by the divalent cation forced water molecules and humic functional groups into rigid positions near the Ca^{2+} and discouraged subtle changes to the structure of the polyanion that would lead to the formation of H-bonds. Analysis of sorption and desorption of probe molecules by cation-saturated humic acids [7] indicates that the identity of the cation-saturating humic substances can affect sorption of nonionic organic compounds via both H-bonding and hydrophobic mechanisms.

Plots of Na-O and Ca-O RDFs provided information concerning the average coordination states of these cations (Fig. 3). The Na-O$_{total}$ profile indicated substantial coordination at Na-O distances of 2 Å or less, and the relative heights of the Na-O$_{carboxylate}$ and Na-O$_{water}$ profiles suggested that most of the O involved in these complexes was part of carboxylate functional groups. The CN values (Table 2) were calculated using a maximum r-value (ρ) for inner-sphere coordination of 2.6 Å. Water O represented more than two-thirds of the average 2.66 O surrounding Na$^+$, whereas carboxylate O represented just under a quarter of this value. The first peak of the Ca-O$_{total}$ RDF occurred at a slightly higher r-value than that seen in the Na-DOM system and also resulted, primarily, from coordination with carboxylate O (Fig. 3). Although Ca^{2+} and Na$^+$ have similar radii, the higher charge of Ca^{2+} attracted more O atoms within a distance of 2.8 Å, and this crowding discouraged occupation of positions closer to the cation. The Ca-O CN values (Table 2) reflect the high O coordination of these cations relative to Na$^+$. The Ca^{2+} were coordinated to a total of 4.15 O on average, including 1.29 carboxylate O, demonstrating significant inner-sphere coordination with organic functional groups. The Ca^{2+} were coordinated to more water O than the Na$^+$ were because of the larger energy of hydration of the divalent cation. Organic, noncarboxylate O functional groups provided a similar amount of inner-sphere coordination to both cations.

The average number of O atoms surrounding Na$^+$ and Ca^{2+}
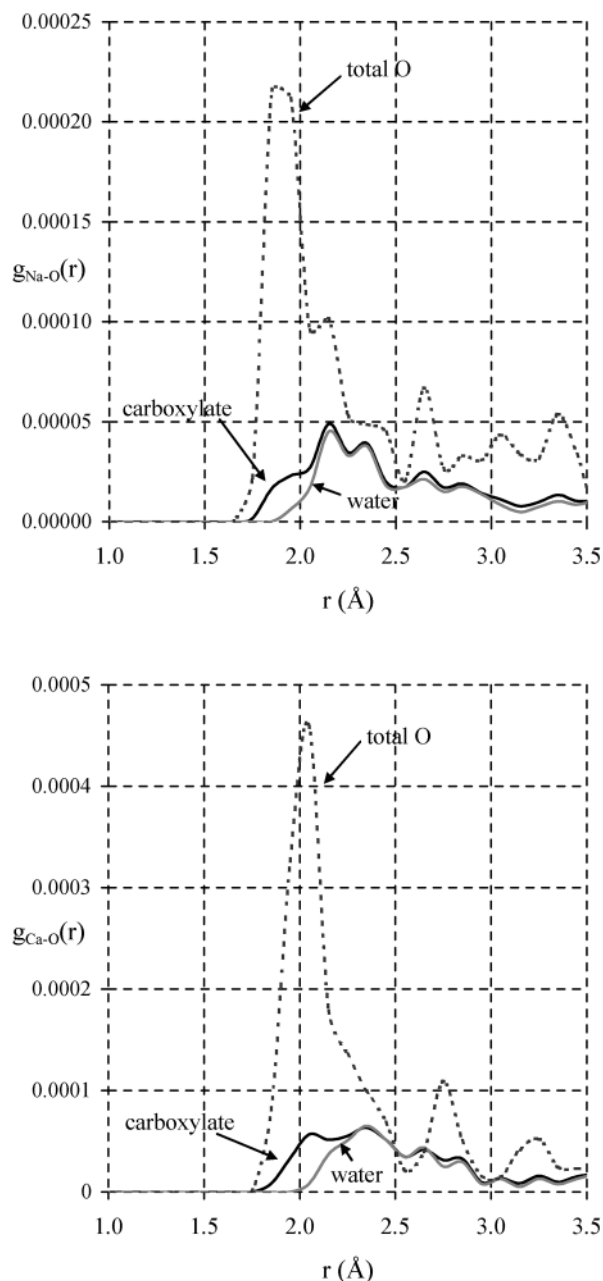
Fig. 3. Radial distribution functions (RDFs) between the cation and total O (gray, dashed line), carboxylate O (black, solid line), and water O (gray, solid line) for Na- and Ca–dissolved organic matter (DOM; top and bottom, respectively) hydrates. No normalization is applied to these RDFs, and as r approaches a value equal to half that of the longest dimension of the system, $g(r)$ approaches zero. Peak heights in the Na-DOM system are roughly half those in the Ca-DOM system, because approximately twice as many Na$^+$ as Ca^{2+} were present.

Table 2. Cation coordination numbers for Na- and Ca-dissolved organic matter hydrates

Cation-O pairs	Na$^+$	Ca^{2+}
Total O	2.66	4.15
Carboxylate O	0.65	1.29
Water O	1.84	2.70
Other O	0.17	0.16

was lower than the experimentally determined aqueous CN values of approximately six for both cations [36]. Restrictions in the stereochemical environment of cations experiencing inner-sphere coordination with DOM, or complexation, may have resulted in substantially reduced coordination overall. Cations directly coordinated to carboxylate O were located close to other organic moieties as well. Further coordination of these cations by water molecules would be restricted to positions not impinged on by fragments of the DOM molecule. The longer average Ca-O coordination distance described above, created through packing of O around the more hydrophilic divalent cation, reduced the effect of stereochemical barriers to coordination for Ca^{2+} relative to Na^+. It is possible that the method used to create these cation-saturated systems also contributed to the low CN values of the cations relative to experimental values. To reduce the calculations needed to titrate the DOM molecule, the only water present in the systems was the six molecules associated with each cation added. Within this relatively dehydrated environment, hydrophilic functional groups of the DOM may have drawn water molecules away from cations. A layer of water molecules was placed around the cation-saturated DOM polyanion after the titration was complete, but a bias favoring lower coordination of cations may have been introduced by these initial conditions. A similar titration procedure performed on a hydrated DOM molecule might result in cations with larger CN values.

With a carboxylate O CN value of 0.65, Na^+ experienced approximately half the complexation of Ca^{2+}, with its corresponding value of 1.29. Monovalent cations are expected to participate in fewer inner-sphere associations with carboxylate groups compared to divalent cations [6], but even this relatively low amount of Na^+ complexation is inconsistent with currently accepted models of cation complexation by humic substances, which suggest that Na^+ interacts with natural organic matter primarily as a diffuse layer of fully hydrated cations removed from specific organic charge sites [6]. Acidimetric titration experiments show that the amount of cation associated with a humic acid is dependent on pH only, not on the concentration of Na^+ in solution, supporting the prevalence of a nonspecific charge neutralization interaction rather than direct organic complexation [8]. The model titration procedure used for these simulations may produce results favoring organic complexation interactions over more distant, charge-neutralization activity, because cations are placed near newly deprotonated carboxylate groups at the beginning of each step in the sequence. The relatively dehydrated conditions during titration described above may encourage formation of inner-sphere complexes as well.

In contrast, the complexation behavior of Ca^{2+} observed in these simulations is consistent with currently accepted models of cation complexation by humic substances, which suggest divalent cations can form inner-sphere complexes with humic carboxylate groups [6]. Conductimetric titration of a humic acid with $Ca(OH)_2$ [9] revealed a large portion of the titration curve for which additions of Ca^{2+} produced almost no increase in conductivity, which is evidence for strong association between the divalent cation and the organic molecules, as seen in the simulations. The same titration performed with NaOH provided further evidence for minimal strong binding of Na^+ to humic acid [9]. Infrared spectra of dehydrated Ca-DOM samples feature a reduction in the carboxyl peak, coupled with an increase in the carboxylate peak, indicating that the cations interact with carboxylate groups directly [48,49]. However,
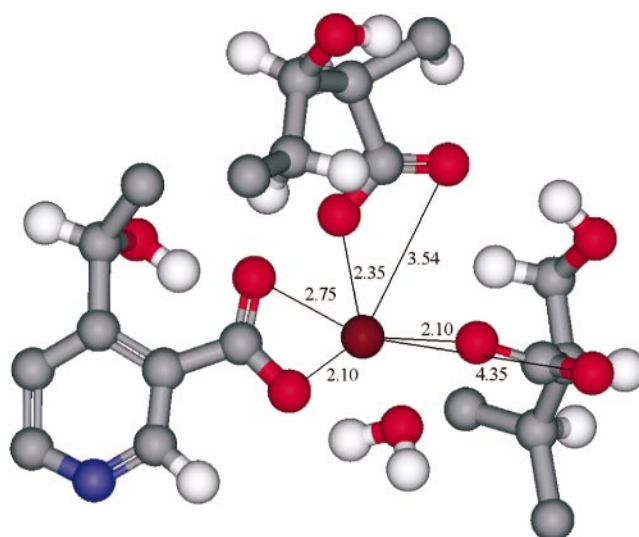
Fig. 4. A portion of the Ca–dissolved organic matter structure featuring a Ca^{2+} doubly inner-sphere coordinated to one carboxylate (left) and singly inner-sphere coordinated to two others (top and right). Gray spheres represent C, red spheres O, white spheres H, blue sphere N, and the brown sphere Ca^{2+}. Measurements indicate distances between atoms (Å).

spectra of partially hydrated Ca-DOM samples do not exhibit this pattern [50], suggesting that Ca^{2+} may not participate primarily in inner-sphere complexes when more water molecules are present. Similar caution concerning the effect of water content must apply to the results of these simulations. The limited number of water molecules present during the initial deprotonation and cation-saturation sequence may have created a bias favoring formation of inner-sphere complexes.

Examination of the local environment of each cation revealed a complex view of cation–carboxylate interactions. The Na-DOM hydrate contained 9 Na^+ that were doubly inner-sphere coordinated to carboxylate groups and 34 that were singly inner-sphere coordinated. Two of the former and eight of the latter cations were singly inner-sphere coordinated with an O of another carboxylate group as well. Neighboring carboxylate groups attached to benzene rings were capable of capturing Na^+ via separate inner-sphere coordination interactions, contributing to a preference for benzene carboxylates to form inner-sphere associations. The 34 remaining Na^+ were in outer-sphere positions relative to carboxylate groups. Two of these cations were more than 6 Å away from the nearest carboxylate, indicating transition from an outer-sphere association to a more independent existence within the shell of water surrounding the deprotonated DOM molecule.

Evaluation of the local cation environments of the Ca-DOM hydrate uncovered greater variation in the coordination states adopted by Ca^{2+}. Three of these cations were doubly inner-sphere coordinated to one carboxylate group and singly inner-sphere coordinated to two others (Fig. 4). Two Ca^{2+} were doubly inner-sphere coordinated to one carboxylate group and singly inner-sphere coordinated to one other. Nine cations participated in doubly inner-sphere coordination complexes with just one carboxylate group. Two Ca^{2+} were singly inner-sphere coordinated to two carboxylate groups simultaneously, whereas 13 Ca^{2+} were singly inner-sphere coordinated to just one carboxylate group. The Ca-DOM hydrate featured a total of 15 doubly inner-sphere complexes and 24 singly inner-sphere complexes. Relative to alkyl carboxylate groups, aromatic car-

boxylate groups were more likely to form doubly inner-sphere complexes. A total of just 10 of the 38 Ca^{2+} were associated with the DOM molecule through outer-sphere complexes, and none of these displayed the drift into the water shell seen in the Na-DOM hydrate.

Comparison of the cation complexation occurring in the Na- and Ca-DOM hydrates indicates that Na^+ is more weakly bound to the DOM polyanion than Ca^{2+}. Nearly half the Na^+ interacted with the organic molecule via outer-sphere associations, as opposed to stronger inner-sphere complexes, whereas just more than a quarter of the Ca^{2+} took part in outer-sphere associations. All the outer-sphere Ca^{2+} were located within 6 Å of a carboxylate O, whereas two of the outer-sphere Na^+ occupied positions at distances greater than 6 Å, suggesting they were associated less directly with the DOM. A survey of exchange movement indicated that 42 Na^+, or more than half the cations present, moved away from the carboxylate groups to which they were originally paired. Within the Ca-DOM hydrate, exchange of the original carboxylate group coordinated to a specific Ca^{2+} for another occurred for only 22 of the 76 initial associations created during titration (two for each Ca^{2+} present, because originally, each was placed near two carboxylate groups). This movement is evidence of the weaker interaction of Na^+ with carboxylate groups as well as its greater mobility in the hydrated organic system compared to Ca^{2+}. Although the titration procedure used to model the Na-DOM system may have favored the formation of inner-sphere coordinated complexes, it is evident that Na^+ was not as strongly bound to the organic polyanion as Ca^{2+} was, a trend that is consistent with current theory [6] and experimental evidence [8,9]. In contrast to Na^+, Ca^{2+} was more likely to be doubly inner-sphere coordinated with carboxylate groups and to remain near both the DOM molecule and the carboxylate groups associated with initial placement during titration, which are characteristics that support the idea of a tightly bound cation.

CONCLUSION

The DOM molecule, designed by Schulten [16] and modeled using the COMPASS force field, displayed physical and chemical characteristics consistent with experimental data. The model humic molecule reproduced a value for dry bulk density within the range of those determined for humic substances and a value for the Hildebrand solubility parameter just less than those estimated from experimental measurements. Explorations of a hydrated DOM system indicated that the subtle structural reorganization triggered by solvation was enough to disrupt numerous intramolecular H-bonds, despite the fact that few water molecules penetrated the organic matrix. The radius of gyration of the hydrated DOM molecule was consistent with those measured for aquatic humic substances.

To examine the structure of humic substances under pH conditions closer to neutral, a novel method of stepwise titration was developed in which hydrated cations were placed near deprotonated carboxyl functional groups. Both Na- and Ca-DOM structures created in this manner were more porous and featured more DOM–water H-bonds than the protonated hydrate. The Ca^{2+} displayed stronger organic complexation and reduced mobility relative to the Na^+ as well as a greater level of hydration by water molecules, all of which result from its greater charge.

The DOM molecule, as simulated by the COMPASS force field, is a potentially valuable tool for investigating the structure and function of aqueous humic molecules under acidic and near-neutral pH conditions. The work presented here is the first rigorous computational exploration regarding the behavior of a model humic molecule under a variety of physical conditions that are typical of soil and water systems. Broad comparison of the properties of model molecules and natural humic fractions is an essential step toward a mechanistic understanding of processes involving humic substances. Further studies using other model molecules should lead to improved three-dimensional organic structures that capture functional qualities of humic materials and can be used to make predictions about contaminant mobility in natural systems.

REFERENCES

1. Sutton R, Sposito G. 2001. Molecular simulation of interlayer structure and dynamics in 12.4 Å Cs-smectite hydrates. *J Colloid Interface Sci* 237:174–184.
2. Zaidan OF, Greathouse JA, Pabalan RT. 2003. Monte Carlo and molecular dynamics simulation of uranyl adsorption on montmorillonite clay. *Clays and Clay Minerals* 51:372–381.
3. Teppen BJ, Yu C-H, Miller DM, Schafer L. 1998. Molecular dynamics simulations of sorption of organic compounds at the clay mineral/aqueous solution interface. *Journal of Computational Chemistry* 19:144–153.
4. Bailey GW, Akim LG, Shevchenko SM. 2001. Predicting chemical reactivity of humic substances for minerals and xenobiotics: Use of computational chemistry, scanning probe microscopy and virtual reality. In Clapp CE, Hayes MHB, Senesi N, Bloom PR, Jardine PM, eds, *Humic Substances and Chemical Contaminants.* Soil Science Society of America, Madison, WI, pp 41–72.
5. Stevenson FJ. 1994. *Humus Chemistry: Genesis, Composition, Reactions,* 2nd ed. John Wiley, New York, NY, USA.
6. Tipping E. 2002. *Cation Binding by Humic Substances.* Cambridge University Press, Cambridge, UK.
7. Yuan G, Xing B. 2001. Effects of metal cations on sorption and desorption of organic compounds in humic acids. *Soil Sci* 166:107–115.
8. Bonn BA, Fish W. 1993. Measurement of electrostatic and site-specific associations of alkali metal cations with humic acid. *J Soil Sci* 44:335–345.
9. Van den Hoop MAGT, van Leeuwen HP. 1990. Study of the polyelectrolyte properties of humic acids by conductimetric titration. *Anal Chim Acta* 232:141–148.
10. Steelink C. 1985. Implications of elemental characteristics of humic substances. In Aiken GR, McKnight DM, Wershaw RL, eds, *Humic Substances in Soil, Sediment, and Water.* John Wiley, New York, NY, USA, pp 457–476.
11. Davies G, Fataftah A, Cherkasskiy A, Ghabbour EA, Radwan A, Jansen SA, Kolla S, Paciolla MD, Sein LT, Buermann W, Balasubramanian M, Budnick J, Xing B. 1997. Tight metal binding by humic acids and its role in biomineralization. *J Chem Soc Dalton Trans* 1997:4047–4060.
12. Leenheer JA. 1994. Chemistry of dissolved organic matter in rivers, lakes, and reservoirs. In Baker LA, ed, *Environmental Chemistry of Lakes and Reservoirs.* American Chemical Society, Washington, DC, pp 195–221.
13. Leenheer JA, McKnight DM, Thurman EM, MacCarthy P. 1989. Structural components and proposed structural models of fulvic acid from the Suwannee River. In Averett RC, Leenheer JA, McKnight DM, Thorn KA, eds, *Humic Substances in the Su-*

wannee River, Georgia: Interactions, Properties, and Proposed Structures. U.S. Geological Survey, Denver, CO, pp 335–359.

14. Leenheer JA, Wershaw RL, Reddy MM. 1995. Strong-acid, carboxyl-group structures in fulvic acid from the Suwannee River, Georgia. 2. Major structures. *Environ Sci Technol* 29:399–405.

15. Schulten H-R, Schnitzer M. 1993. A state of the art structural concept for humic substances. *Naturwissenschaften* 80:29–30.

16. Schulten H-R. 1999. Analytical pyrolysis and computational chemistry of aquatic humic substances and dissolved organic matter. *J Anal Appl Pyrolysis* 49:385–415.

17. Shevchenko SM, Bailey GW. 1996. The mystery of the lignin-carbohydrate complex: A computational approach. *Journal of Molecular Structure* 364:197–208.

18. Diallo MS, Faulon J-L, Goddard WA, Johnson JH. 2001. Binding of hydrophobic organic compounds to dissolved humic substances: A predictive approach based on computer assisted structure elucidation, atomistic simulations and Flory–Huggins solution theory. In Ghabbour EA, Davies G, eds, *Humic Substances: Structures, Models, and Functions.* Royal Society of Chemistry, London, UK, pp 221–237.

19. Diallo MS, Simpson A, Gassman P, Faulon JL, Johnson JH, Goddard WA, Hatcher PG. 2003. 3-D structural modeling of humic acids through experimental characterization, computer assisted structure elucidation and atomistic simulations. 1. Chelsea soil humic acid. *Environ Sci Technol* 37:1783–1793.

20. Kubicki JD, Apitz SE. 1999. Models of natural organic matter and interactions with organic contaminants. *Organic Geochemistry* 30:911–927.

21. Jansen SA, Malaty M, Nwabara S, Johnson E, Ghabbour E, Davies G, Varnum JM. 1996. Structural modeling in humic acids. *Materials Science and Engineering C* 4:175–179.

22. Schulten H-R. 1999. Interactions of dissolved organic matter with xenobiotic compounds: Molecular modeling in water. *Environ Toxicol Chem* 18:1643–1655.

23. Bruccoleri AG, Sorenson BT, Langford CH. 2001. Molecular modeling of humic structures. In Ghabbour EA, Davies G, eds, *Humic Substances: Structures, Models and Functions.* Royal Society of Chemistry, Cambridge, UK, pp 193–208.

24. Accelrys. 2001. *Cerius² Release 4.6.* San Diego, CA, USA.

25. Sun H. 1998. COMPASS: An ab initio force-field optimized for condensed-phase applications—Overview with details on alkane and benzene compounds. *J Phys Chem B* 102:7338–7364.

26. Kubicki JD. 2000. Molecular mechanics and quantum mechanical modeling of hexane soot structure and interactions with pyrene. *Geochemical Transactions* 7:41–46.

27. Kubicki JD, Trout CC. 2003. Molecular modeling of fulvic and humic acids: Charging effects and interactions with Al^{3+}, benzene, and pyridine. In Selim HM, Kingery WL, eds, *Geochemical and Hydrological Reactivity of Heavy Metals in Soil.* Lewis, Boca Raton, FL, USA, pp 113–143.

28. Allen MP, Tildesley DJ. 1987. *Computer Simulation of Liquids.* Oxford University Press, Oxford, UK.

29. Schnitzer M, Schulten H-R. 1998. New ideas on the chemical make-up of soil humic and fulvic acids. In Huang PM, Sparks DL, Boyds SA, eds, *Future Prospects for Soil Chemistry.* Soil Science Society of America, Madison, WI, pp 153–177.

30. Sutton R. 2004. A molecular modeling exploration of smectite interlayers as adsorption sites for inorganic and organic molecules. PhD thesis. University of California at Berkeley, Berkeley, CA, USA.

31. Beveridge DL, Mezei M, Mehrotra PK, Marchese FT, Ravi-Shanker G, Vasu T, Swaminathan S. 1983. Monte Carlo computer simulation studies of the equilibrium properties and structure of liquid water. In Haile JM, Mansoori, GA, eds, *Molecular-Based Study of Fluids.* American Chemical Society, Washington, DC, pp 297–351.

32. Soper AK, Phillips MG. 1986. A new determination of the structure of water at 25°C. *Chemical Physics* 107:47–60.

33. Akim LG, Bailey GW, Shevchenko SM. 1998. A computation chemistry approach to study the interactions of humic substances with mineral surfaces. In Davies G, Ghabbour EA, eds, *Humic Substances: Structures, Properties, and Uses.* Royal Society of Chemistry, Cambridge, UK, pp 133–145.

34. Sein LT, Varnum JM, Jansen SA. 1999. Conformational modeling of a new building block of humic acid: Approaches to the lowest energy conformer. *Environ Sci Technol* 33:546–552.

35. Shevchenko SM, Bailey GW, Akim LG. 1999. The conformational dynamics of humic polyanions in model organic and organo-mineral aggregates. *Journal of Molecular Structure* 460: 179–190.

36. Ohtaki H, Radnai T. 1993. Structure and dynamics of hydrated ions. *Chem Rev* 93:1157–1204.

37. Von Wandruszka R, Engebretson RR, Yates LM. 1999. Humic acid pseudomicelles in dilute aqueous solution: Fluorescence and surface tension measurements. In Ghabbour EA, Davies G, eds, *Understanding Humic Substances: Advanced Methods, Properties, and Applications.* Royal Society of Chemistry, Cambridge, UK, pp 79–85.

38. Vachette P, Svergun D. 2000. Small-angle x-ray scattering by solutions of biological macromolecules. In Franchon E, Geissler E, Hodeau J-L, Regnard J-R, Timmins PA, eds, *Structure and Dynamics of Biomolecules: Neutron and Synchrotron Radiation for Condensed Matter Studies.* Oxford University Press, Oxford, UK, pp 199–237.

39. Sposito G, Skipper NT, Sutton R, Park S-H, Soper AK, Greathouse JA. 1999. Surface geochemistry of the clay minerals. *Proc Natl Acad Sci U S A* 96:3358–3364.

40. Sposito G, Park SH, Sutton R. 1999. Monte Carlo simulation of the total radial distribution function for interlayer water in sodium and potassium montmorillonites. *Clays and Clay Minerals* 47: 192–200.

41. Maguna FP, Núñez MB, Okulik NB, Castro EA. 2003. Improved QSAR analysis of the toxicity of aliphatic carboxylic acids. *Russian Journal of General Chemistry* 73:1792–1798.

42. Kopinke F-D, Porschmann J, Stottmeister U. 1995. Sorption of organic pollutants on anthropogenic humic matter. *Environ Sci Technol* 29:941–950.

43. Thurman EM, Wershaw RL, Malcolm RL, Pinckney DJ. 1982. Molecular size of aquatic humic substances. *Organic Geochemistry* 4:27–35.

44. Aiken GR, Brown PA, Noyes TI, Pinckney DJ. 1989. Molecular size and weight of fulvic and humic acids from the Suwannee River. In Averett RC, Leenheer JA, McKnight DM, Thorn KA, eds, *Humic Substances in the Suwannee River, Georgia: Interactions, Properties, and Proposed Structure.* U.S. Geological Survey, Denver, CO, pp 163–178.

45. Wershaw RL, Burcar PJ, Sutula CL, Wiginton BJ. 1967. Sodium humate solution studied with small-angle x-ray scattering. *Science* 157:1429–1431.

46. Graber ER, Borisover MD. 1998. Hydration-facilitated sorption of specifically interacting organic compounds by model soil organic matter. *Environ Sci Technol* 32:258–263.

47. Maurice PA, Namjesnik-Dejanovic K. 1999. Aggregate structures of sorbed humic substances observed in aqueous solutions. *Environ Sci Technol* 33:1538–1541.

48. Griffith SM, Schnitzer M. 1975. The isolation and characterization of stable metal-organic complexes from tropical volcanic soils. *Soil Sci* 120:126–131.

49. Alberts JJ, Filip Z. 1998. Metal binding in estuarine humic and fulvic acids: FTIR analysis of humic acid–metal complexes. *Environ Technol* 19:923–931.

50. Bonn BA. 1992. Interactions of a soil humic acid with alkali metal cations and alkaline earth metal cations. PhD thesis. Lewis and Clark College, Portland, OR, USA.